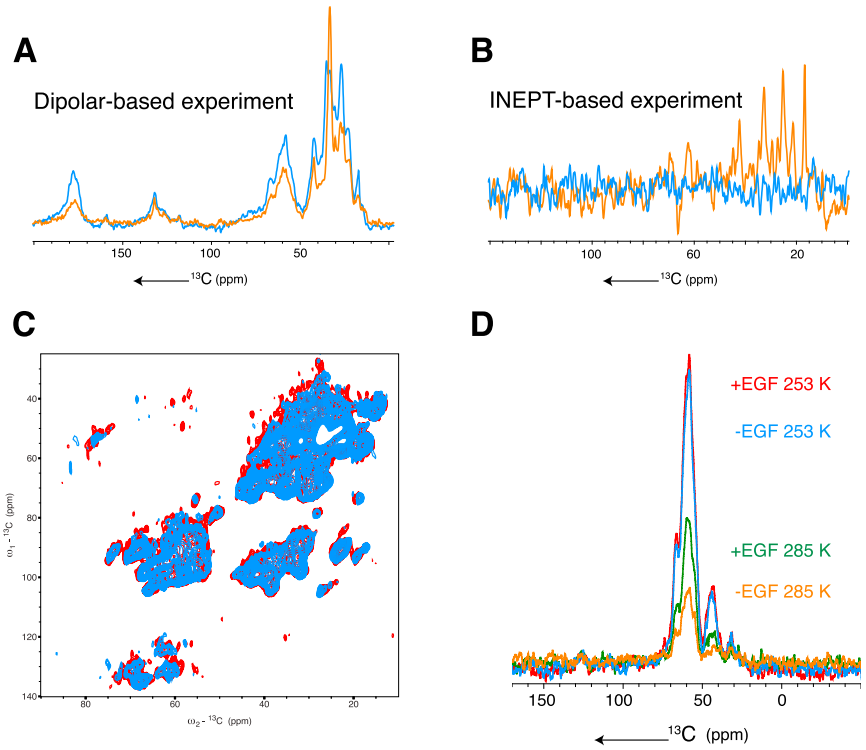

Figure S1. Temperature Dependence of One- and Two-Dimensional ssNMR Experiments Using [^{13}C, ^{15}N]-Labeled A431 Plasma Membrane Vesicles with and without EGF, Related to Figure 4

(A) ^{13}C CP (cross polarization, which probes the rigid parts of the sample (Pines et al., 1973)) experiment of [^{13}C, ^{15}N]-labeled A431 plasma membrane vesicles without EFG at 253 K (blue) and 285 K (orange).

(B) INEPT-based (See (Morris and Freeman, 1979) experiment, to probe the mobile parts of the sample of [^{13}C, ^{15}N]-labeled A431 plasma membrane vesicles without EFG at 253 K (blue) and 285 K (orange).

(C) 2D ^{13}C,^{13}C) double-quantum / single-quantum experiment (DQSQ) with (red) and without (blue) EGF performed at 253 K.

(D) First increment of 2D NCa of [^{13}C, ^{15}N]-labeled A431 plasma membrane vesicles without EGF (blue at 253 K and orange at 285 K) and with EGF (red at 253 K and green at 285 K).

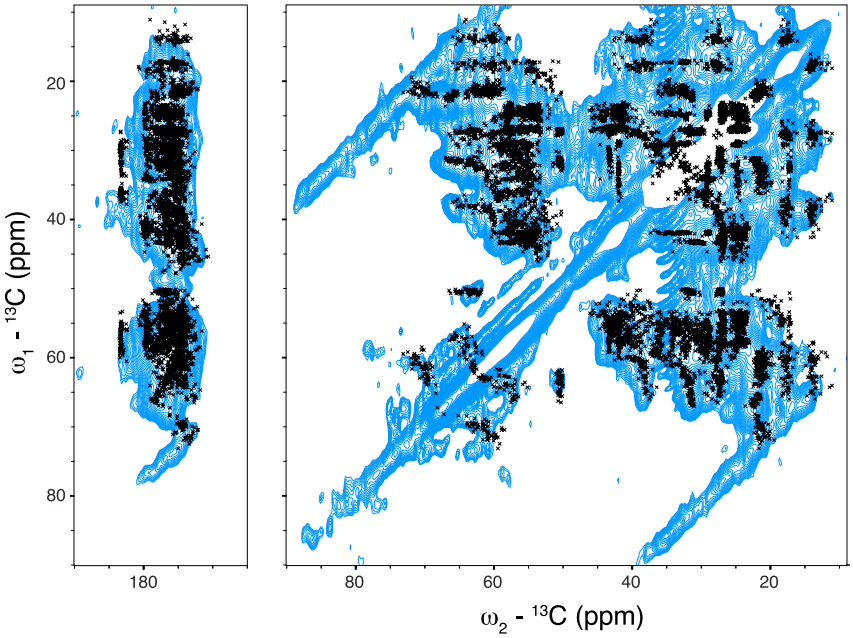

Figure S2. Comparison of ssNMR Spectra of [^{13}C, ^{15}N]-Labeled A431 Membrane Vesicles at Low Temperatures to EGFR Chemical-Shift Predictions, Related to Figure 4

The 2D (^{13}C,^{13}C) PARIS experiment was performed at 253 K. Black crosses represent FANDAS (Gradmann et al., 2012) predictions of EGFR based on the different available structures and assuming random-coil chemical shifts for the C-terminal region (CT). Note that the peaks at ~70 ppm are stemming from lipids. As mentioned in the section Materials and Methods, EGFR samples were prepared using unlabeled Glutamine, Tryptophan and Cysteine amino acids and, correspondingly, were not included in the FANDAS correlation map. FANDAS predictions were made based on the following structures: 1NQL (Extracellular inactive), 2M20 (Transmembrane domain), 2M20 (Juxtamembrane), 1M14 (Kinase domain), 1M14 (part of the C-terminal tail).

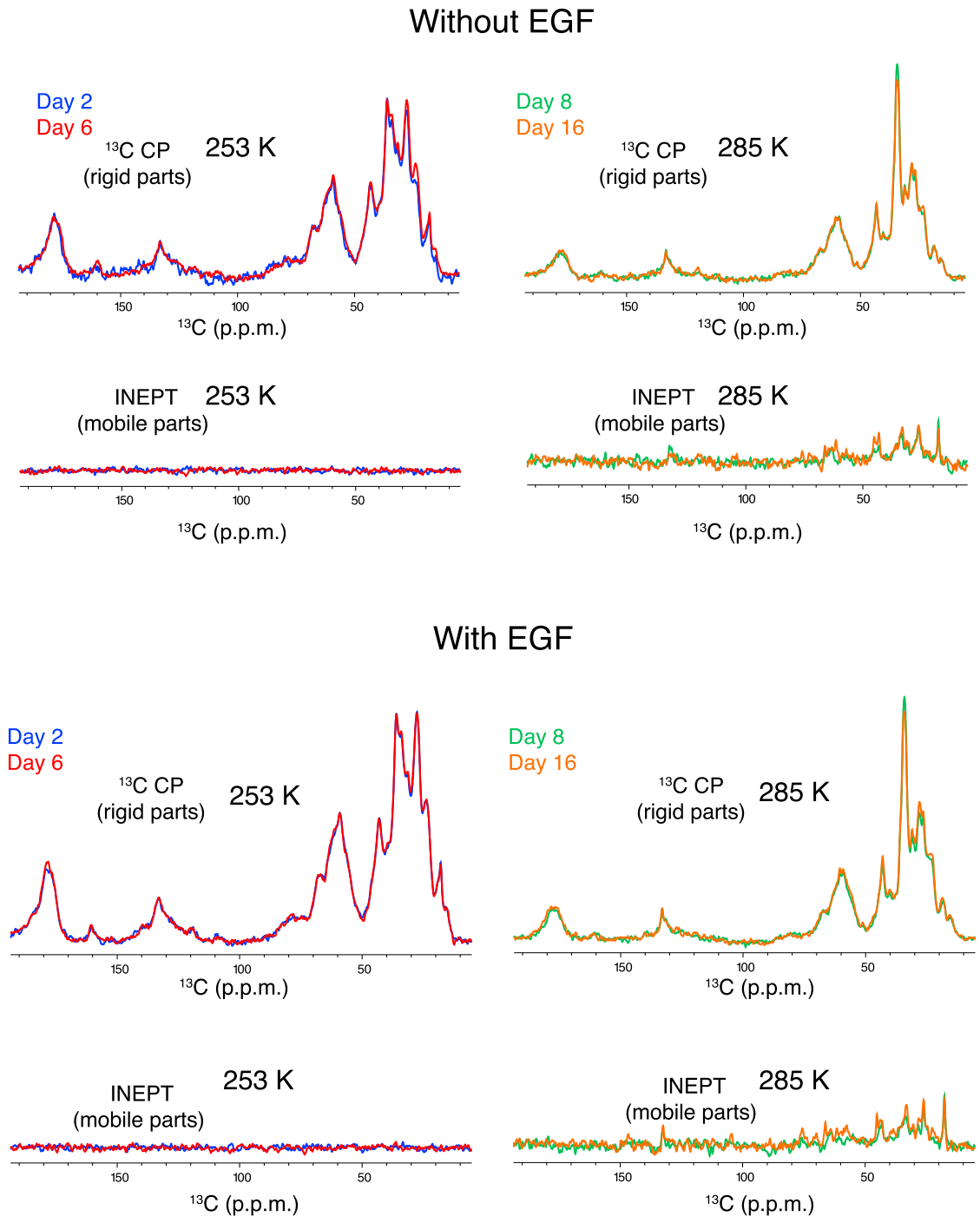

Figure S3. ssNMR Signal Patterns for Extended Measurement Periods, Related to Figure 4

1D ^{13}C CP and INEPT on [^{13}C, ^{15}N]-labeled A431 vesicles with and without EGF performed during the course of 2D experiments. At the end of measurements (day 16), both samples showed the same profile as in the beginning of the measurements. Data were recorded on a 700 MHz NMR instrument.

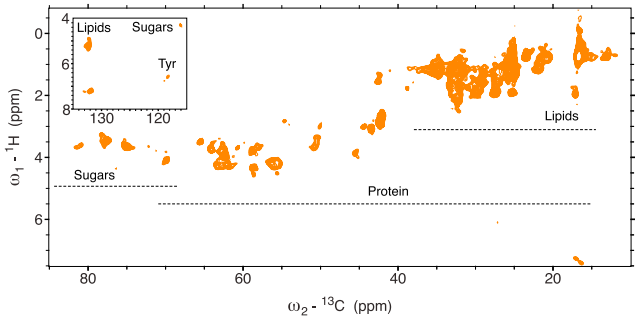

Figure S4. Mobile Molecules Appear at Higher Temperature in 2D ssNMR Data, Related to Figure 4

2D INEPT experiment (See Andronesi et al., 2005) of [^{13}C, ^{15}N]-labeled A431 membrane vesicles without EGF performed at 285 K showing mobile molecular components.

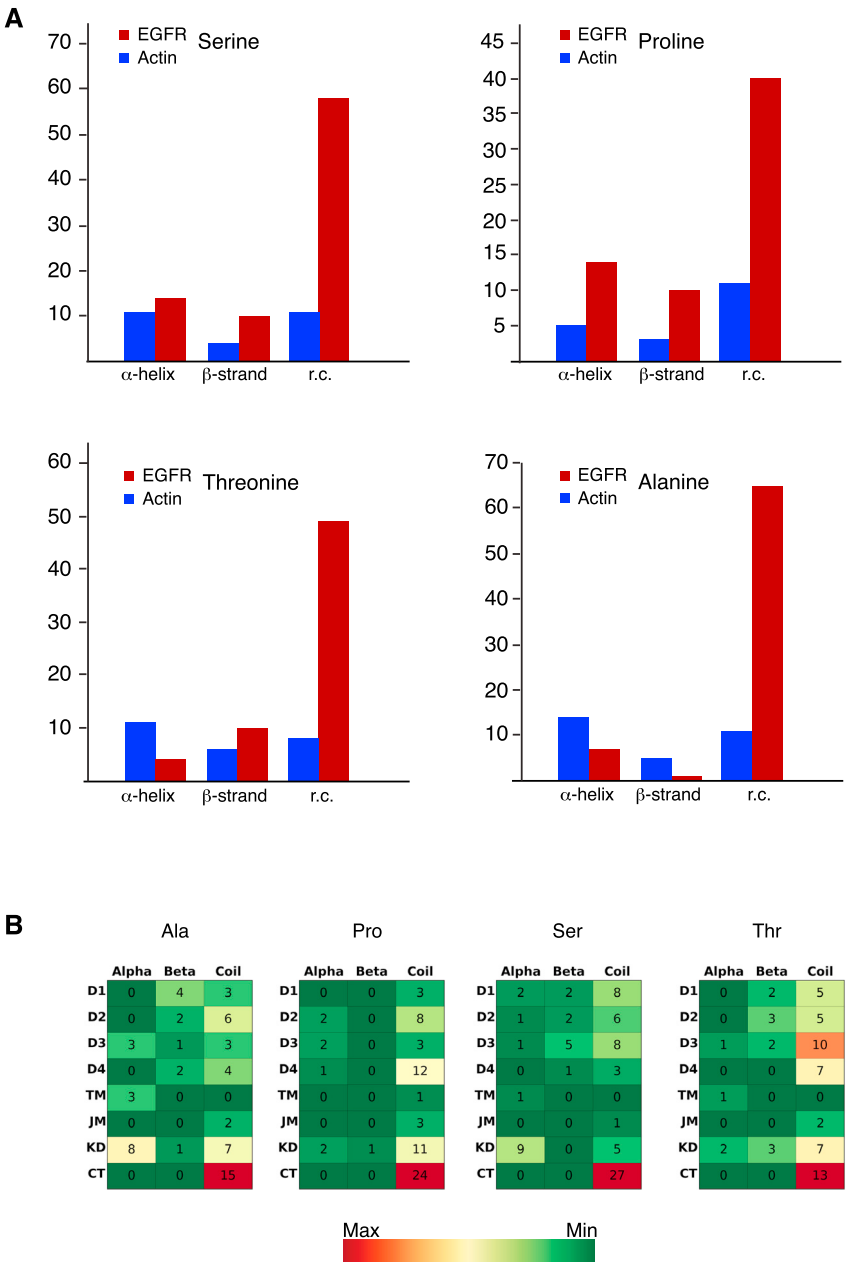

Figure S5. Secondary-Structure Analysis of EGFR, Actin, and EGFR Domains, Related to Figures 4 and 5

(A) Comparison of the distribution of Ser, Thr, Pro and Ala residue in different secondary structures between EGFR (red) and Actin (blue). The y axis represents the number of each amino acid in the correspondent secondary structure.

(B) Heatmaps of the distribution of Ala, Pro, Ser and Thr residues in EGFR for the three secondary structure elements (α-helix, β strand and random coil). Red and green stand for the highest and lowest numbers of occurrence, respectively.

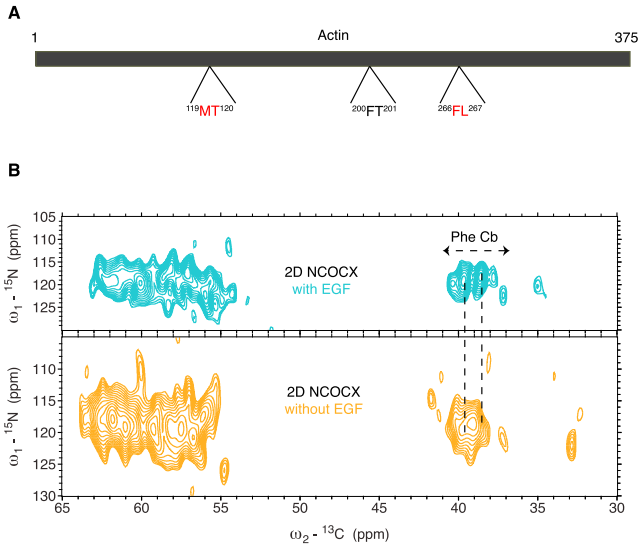

Figure S6. Sequential Correlations Predicted for Actin in the MFTL-Labeled A431 Membrane Vesicles and High-Field DNP Data, Related to Figure 5

(A) highlights the three expected correlations of Actin in the MFTL labeled A431 membrane vesicles.

(B) 2D NCOCX of MFTL labeled A431 vesicles with (cyan) and without (orange) EGF performed on a 800 MHz DNP machine (Koers et al., 2014). Dotted lines connect the Cb region of Phe in both spectra.